Soft *Listeria*: Actin-based propulsion of liquid drops

Hakim Boukellal,[1] Otger Campás,[1,2] Jean-François Joanny,[1] Jacques Prost,[1,3] and Cécile Sykes[1]

[1]*Institut Curie, UMR 168, 26 rue d'Ulm, F-75248 Paris Cedex 05, France*
[2]*Department d'ECM, Universitat de Barcelona, Avinguda Diagonal 647, E-08028 Barcelona, Spain*
[3]*ESPCI, 10 rue Vauquelin, F-75231 Paris Cedex 05, France*
(Received 5 May 2003; published 2 June 2004)

We study the motion of oil drops propelled by actin polymerization in cell extracts. Drops deform and acquire a pearlike shape under the action of the elastic stresses exerted by the actin comet, a tail of cross-linked actin filaments. We solve this free boundary problem and calculate the drop shape taking into account the elasticity of the actin gel and the variation of the polymerization velocity with normal stress. The pressure balance on the liquid drop imposes a zero propulsive force if gradients in surface tension or internal pressure are not taken into account. Quantitative parameters of actin polymerization are obtained by fitting theory to experiment.

PACS number(s): 87.15.$-$v, 87.10.$+$e, 87.14.$-$g

Actin polymerization is a key element in the motility of most cells and bacteria. The bacteria *Listeria monocytogenes* are propelled inside cells by the growth of a soft elastic comet made of a filamentous actin network. Actin polymerizes at the back of the advancing bacterium. The biochemistry of the comet formation is now well understood [1]. Theoretical approaches have been proposed to explain the physical mechanism of force production. They differ by the scale at which they describe the mechanism. Molecular models by Mogilner *et al.* [2] consider the Brownian flexibility of growing actin filaments, whereas Carlsson [3] concentrates on the effect of branching and growth of the actin network. Gerbal *et al.* [4] analyze at a mesoscopic scale the elastic stresses exerted by the deformed comet gel on the bacterium resulting in the propulsive force [5].

A further step in understanding the propulsion mechanism is provided by the study of biomimetic experimental systems where *Listeria* are replaced by solid spherical beads on which actin polymerization promoters [6–9] are attached. These beads mimic closely the natural propulsion mechanism of *Listeria* with comet tail formation, after the breaking of the initial spherical symmetry [6,10]. Biomimetic systems allow for a systematic variation of the parameters and thus for a quantitative comparison to theory.

The aim of this paper is to demonstrate both theoretically and experimentally the mechanism of force production due to the elastic stresses exerted by the actin comet gel. A newly designed experimental system is made of oil drops with actin polymerization promoters attached on their surface. Once placed in cell extracts, such an oil drop moves by actin polymerization and deforms under the action of the elastic stresses exerted by the gel. The same squeezing effect is observed on endosomes [11] driven by actin comets and synthetic vesicles covered with the bacterial protein ActA [12,13]. However, for liquid drops, the knowledge of the surface tension and the constant volume allow for a quantitative analysis of the observed shape and thus the determination of the elastic stress distribution on the drop surface.

An emulsion of oil drops is obtained by sonicating (5 sec, 90 W) a mixture of edible oil, Isio4, and buffer (2.3% oil in borate buffer 100 mM, pH 8.5). The actin polymerization promoter VCA is the C-terminal domain of the Wiskott-Aldrich syndrom protein (WASP) that interacts with the Arp 2/3 complex and actin monomer, and purified as described in Fradelizi *et al.* [14]. VCA is adsorbed onto the oil drops by incubating $10\,\mu$l of the emulsion with a 0.2 mg/ml VCA solution in borate buffer. A volume of $0.2\,\mu$l of the emulsion coated with VCA is added to $15\,\mu$l of HeLa extracts prepared as explained in Noireaux *et al.* [9] with a final protein concentration of 19 mg/ml. As usual the extracts are supplemented with 0.019 mg/ml G-actin, 0.06 mg/ml rhodamin actin, 1 mM ATP, 27 mM creatine phosphate, 1 mM DTT (dithio-threitol).

The sample is observed by bright field or fluorescence microscopy using an Olympus BX51 (Germany) and Metamorph software (Princeton Instruments, USA). The drop radii range from 1.5 to $5.5\,\mu$m. As with *Listeria*, actin polymerizes only at the interface between the drop and the comet and depolymerizes at the back of the comet. When placed in extracts, actin is first polymerized on the drops with a spherical symmetry. After roughly 1 h, symmetry is broken for approximately 70% of the drops. They develop an actin comet, deform into a pearlike shape and move. Smaller drops are less deformed than larger drops. An example of a moving drop is shown in Fig. 1. At the beginning of the experiment, the actin polymerization factor VCA is uniformly distributed around the spherical drop. After deformation of the drop and formation of the comet, fluorescence intensity measurements using FITC (fluorescein isothiocyanate)-labeled VCA [15] show that 90% of the VCA is found on the comet side of the drop, as seen in Fig. 2. This means either that VCA has been displaced from the interface to the bulk of the extract except where the gel is present, or that all VCA has been collected by the gel during the symmetry breaking process. In any event this also means that the VCA surface density is comparable to the density of filament extremities at the surface. The average distance d between filament extremities is larger than the close-packing distance. A lower bound of d is 10 nm. The surface tension change due to the presence of VCA at the interface is then of order $kT/d^2 < 4 \times 10^{-2}$ mN/m, more than 100 times smaller than the oil-extract tension that we measure by the pendant drop method $\gamma_0 = 4 \pm 0.6$ mN/m.
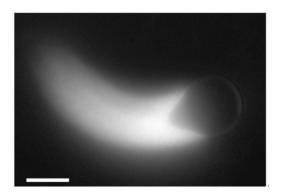
FIG. 1. Oil drop covered with VCA placed in HeLa cell extracts supplemented with Alexa-actin and observed by fluorescence microscopy. The actin comet appears bright. The bar is 4 μm.

The experimental shape of the drop is sketched in Fig. 3. The front part is a spherical cap of radius R not covered by actin. The radius R is different from the radius of the undeformed spherical drop R_0 that fixes the volume $4\pi R_0^3/3$. The back part of the drop, surrounded by the comet, has a blunted conelike shape (rotationally symmetric around the direction of motion). In order to give a theoretical description of the drop shape, we parametrize it by the liquid thickness h and the local angle θ between the tangent to the shape and the direction of motion. The spherical cap and the cone match at the triple line between the drop, the comet, and the surrounding solvent; we call the tangent angle at the contact point θ_m where the corresponding oil thickness is $h_m = R \cos \theta_m$. The pressure inside the drop varies from point to point since the drop motion induces an internal flow. At the interface with the extract, in the spherical part, it is given by Laplace's law $P_{in} = 2\gamma_0/R + P_0$, where P_0 is the pressure in the surrounding liquid. At any point inside the drop, the pressure differs from P_{in} and reads $P = P_{in} + \delta P$. At a point of thickness h the local stress balance along the normal of the drop is given by the local Laplace's law
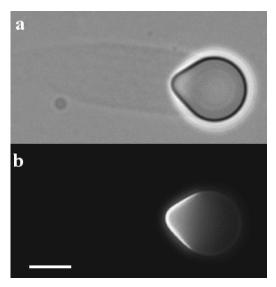

FIG. 2. Oil drop covered with FITC-labeled VCA and placed in HeLa cell extracts observed (a) by bright field microscopy and (b) by fluorescence microscopy. The VCA appears bright. The bar is 3 μm.
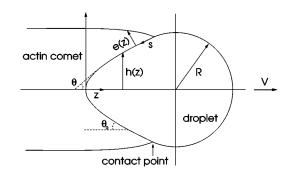

FIG. 3. Sketch of the moving oil drop. For theoretical analysis, the shape is parametrized by the local thickness h and the local angle of the tangent θ.

$$\frac{2\gamma_0}{R} + \delta P(h) = \gamma\left(\frac{\cos \theta(h)}{h} + \frac{d\cos \theta(h)}{dh}\right) - \sigma_{nn}(h) \quad (1)$$

where σ_{nn} is the normal stress at the surface of the comet, exerted by the drop (σ_{nn} is positive, dilative stress, if the comet pulls on the drop and negative, compressive stress, if the comet pushes the drop). Although we argued that the surface tension gradients are small, we consider here that the surface tension $\gamma = \gamma_0 + \delta\gamma(h)$ varies along the interface; it is constant in the spherical part with a value γ_0 and it is continuous at the contact line. The total elastic force F_e exerted by the comet on the drop is obtained by integrating the projection of the normal elastic stress on the direction of motion,

$$F_e/2\pi = \int_0^{h_m} dh\, h\left(\cos\theta\frac{d\delta\gamma}{dh} + \delta P\right). \quad (2)$$

If we ignore both the pressure gradient inside the drop and the surface tension gradient, the propulsive force equals zero. This result holds for any axisymmetric drop shape whatever the elastic stress distribution along the surface, independent of any model for the comet elasticity and the actin polymerization velocity. This hypothesis, used in Refs. [12,13], is unable to produce an estimate of the propulsive force. The important consequence of Eq. (2) is that an experimental measurement of the propulsive force must take into account the surface tension gradient and the flow inside the drop as discussed later.

We now proceed with the determination of the drop shape and the stress distribution. Given that the surface tension variation is small along the drop contour and neglecting hydrodynamic effects, we consider, for local equations, that the surface tension and the internal pressure are constant. The elastic stresses in the gel influence the polymerization kinetics; polymerization is normal to the surface of the drop and it is accelerated by a dilative stress and slowed down by a compressive stress. Classical rate theories [16] predict a polymerization velocity v_p varying as a Boltzmann law

$$v_p(h) = v_p^0 \exp[\sigma_{nn}(h)/\sigma_0], \quad \sigma_0 \equiv kT/a^2\delta \quad (3)$$

where a is the distance between actin polymerization promoters on the drop surface, δ is of the order of the size of an actin monomer, and v_p^0 is the polymerization velocity in the absence of stress.

The last equation determining the shape of the drop is the conservation of the gel volume upon polymerization. In a first approximation, we assume both that the gel density is constant and that the comet is a perfect cylinder. In a steady state, the drop advances at a constant velocity V. The local gel thickness e shown on Fig. 3 is then such that $de/ds = \tan\theta$ where s is the length along the drop contour. With these simplifying approximations, the local polymerization velocity is related to the advancing velocity by $v_p(h) = V\sin\theta(h)$.

This approximation does not allow for the determination of the drop velocity V since the propulsive force vanishes. We thus find a family of solutions for the drop shape parametrized by the advancing velocity. We determine the drop shape using the measured advancing velocity $V = 0.15 \pm 0.03\ \mu\mathrm{m/min}$.

The shape of the comet-drop interface departs from a pure cone when the Boltzmann factor is significantly larger than 1. This defines the size of the blunted region as $\ell \equiv \gamma a^2 \delta / kT$ which leads to $\sigma_0 = \gamma/\ell$. In the following we consider $\varepsilon \equiv \ell/R$ as a small number.

For h of order R, the elastic stress $\sigma_{nn}(h)$ is small and can be neglected. Then Eq. (3) describes a perfect cone with angle $\theta = \theta_0$ such that $V\sin\theta_0 = v_p^0$. This result is independent of the polymerization law giving v_p as a function of $\sigma_{nn}(h)$. The measure of θ_0 thus gives access to the polymerization velocity in the absence of elastic stress.

In the blunted region, h is of order ℓ and we neglect the Laplace pressure term on the left-hand side of Eq. (1). In the vicinity of the rear point, the drop profile is given by $h^2 = 4\ell z/\log(1/\sin\theta_0)$.

The normal stress in the rear region of size ℓ is positive and of order γ/ℓ. At the rear point, $\sigma_{nn}(h=0) = \gamma\log(1/\sin\theta_0)/\ell$. In the conical region, the stress reads at lowest order in ε

$$\sigma_{nn}(h) = (\gamma/R)(-2 + R\cos\theta_0/h). \tag{4}$$

It is positive at the back of the drop (pulling the drop backwards) and negative in the front part of the cone (pushing the drop forwards) as qualitatively observed in Ref. [12]. It vanishes for a thickness $h = (R\cos\theta_0)/2 = h_m/2$. This is in accordance with the prediction made in Ref. [4] that the actin gel could pull at the rear of *Listeria* and explains the pearlike deformation that we now describe quantitatively.

A more detailed description of the drop profile is obtained by solving numerically Eqs. (1) and (3). We use the radius R as a unit length; the drop profile depends on the two dimensionless parameters, ε and $\sin\theta_0 = v_p^0/V$. In Fig. 4 we show a comparison of the calculated and experimental profiles for the drop of Fig. 1. The experimental profile has been digitized and adjusted by a continuous curve. The best fitting parameters are $\varepsilon = 0.049$ and $\sin\theta_0 = 0.58$ ($\theta_0 = 35.6°$); this gives a determination of the length $\ell = 0.125\ \mu\mathrm{m}$, of the stress $\sigma_0 = 32\ \mathrm{nN}/\mu\mathrm{m}^2$, and of the polymerization speed in the absence of stress $v_p^0 = 1.4\ \mathrm{nm/s}$ [17]. The local normal stress is obtained from the experimental drop shape by using Eq. (1) with a constant interfacial tension γ_0 and neglecting
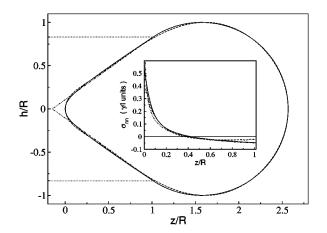

FIG. 4. Calculated drop profile for $\varepsilon = 0.049$ and $\sin\theta_0 = 0.58$ (continuous line) compared to the experimental drop profile (dashed line) and to the zeroth order asymptotic expansion (dash-dotted line). The inset shows the normal stress distribution along the drop surface.

the variation of the internal pressure δP. The length ℓ being constant, smaller drops corresponding to larger ε are less deformed, in agreement with experiments.

In the description proposed so far, the curvature of the interface between the comet and the drop has a discontinuity at the triple line. In the spherical region, the curvature of the interface is $2/R$; in the conical region, the interface is curved only in one direction and the curvature is $1/R$. The local forces normal to the interface are still balanced and the elastic normal stress in the comet at the triple line is $\sigma_{nn}(h_m) = -\gamma/R$ (see the inset of Fig. 4). At the triple line, the gel thickness e vanishes and cannot create a finite stress. This explains why on Fig. 4 the theoretical and experimental normal stresses are in disagreement in the very vicinity of the triple line. We now assume that the gel density remains constant but that the comet shape is not a perfect cylinder in the region close to the triple line. Volume conservation then imposes a polymerization velocity $v_p = V\cos\theta\, de/ds$, where s is the length along the interface. When a gel element is created in a time δt, it is stretched by an amount $\delta u = \delta t(-V\sin\theta + v_p)$; the tensile stresses σ_{ii} in the azimuthal direction ($i = \varphi$) and in the tangential direction along the interface ($i = t$) are then increased. At the level of scaling laws, we write this increase as $d\sigma_{ii}/ds = (E/R_i V\cos\theta)(V\sin\theta - v_p)$, where R_i is the radius of curvature of the interface in the direction i and E an elastic modulus of the comet. In the vicinity of the triple line, we use the thin shell approximation and relate the tensile and normal stresses in the gel $\sigma_{nn} = -e[(\sigma_{tt}/R_t) + (\sigma_{\varphi\varphi}/R_\varphi)]$. In this boundary layer, the two tensile stresses can be considered as constant; the matching to the pearlike shape imposes that the azimuthal tensile stress $\sigma_{\varphi\varphi}$ vanishes. Defining the dimensionless tensile stress $\tilde\sigma_t = \ell\sigma_{tt}/\gamma$, the normal stress in the boundary layer is then calculated as

$$\sigma_{nn} = -\frac{\gamma}{R}\frac{e\tilde\sigma_t}{\ell + e\tilde\sigma_t}. \tag{5}$$

As the thickness of the gel vanishes, the normal stress vanishes as expected. The boundary layer, where the comet is

deformed, has a thickness $\ell/\tilde{\sigma}_t$ of order ℓ and is thus small in the limit where ε is small. When e is large, further away from the triple line, the comet reaches a cylindrical shape and the normal stress is $-\gamma/R$; one can consider the comet as a perfect cylinder as done above.

Our experimental observations on the shape of liquid drops propelled by actin polymerization are well described by the theoretical model based on a local normal force balance and on a Boltzmann variation of the polymerization velocity with normal stress. The results are robust if we use, for the polymerization velocity, the mathematical forms suggested by simulations on flat surfaces [3]. We demonstrate that the elastic propulsive force cannot be calculated from an elastic stress distribution that ignores both pressure variations inside the drop and surface tension gradients. We have estimated the surface tension gradient by assuming that the actin polymerization promoter density profile along the interface follows the gel elastic deformation. This leads to a propulsive force of order $F_e \sim 2\pi\gamma_0\varepsilon_G/E$, where ε_G is the Gibbs elastic modulus of the interface. With reasonable values of the parameters, we find a propulsive force of order 100 pN. This is, however, a lower bound since there could exist other contributions to the surface tension gradient. The advancing velocity of the drop results from a balance between the propulsive force and the friction force between the comet and

the drop but a precise study of the velocity selection will require a more refined analysis.

In our experiments, as well as in Ref. [12], the motion stops when the drop (or the liposome) becomes spherical. The large stress at the back of the drop could lead to "cavitation" or rupture of the links between the drop and the comet. The elastic stresses exerted on the drop then relax and provoke the experimentally observed arrest. We expect the stress distribution to be similar for other types of actin propelled objects such as the bacteria *Listeria* or solid beads. This would explain the observation of hollow comets of *Listeria* [10]. A final output of our analysis is an estimate of the polymerization velocity of an actin gel in the absence of stress and its variation with stress.

[1] T. Pollard, L. Blanchoin, and R. Mullins, Annu. Rev. Biophys. Biomol. Struct. **29**, 545 (2000).

[2] A. Mogilner and G. Oster, Biophys. J. **71**, 3030 (1996); **84**, 1591 (2003).

[3] A.E.Carlsson, Biophys. J. **81**, 1907 (2001).

[4] F. Gerbal, P. Chaikin, Y. Rabin, and J. Prost, Biophys. J. **79**, 2259 (2000).

[5] J. Prost, *The Physics of Listeria Motion in Physics of Biomolecules and Cells*, edited by H. Flyvberg, F.J. Licher, P. Ormos, and F. David, Les Houches Lecture Notes LXXV, (Springer, Berlin), 2002.

[6] A. Bernheim-Groswasser, S. Wiesner, R. Golsteyn, M. Carlier, and C. Sykes, Nature (London) **417**, 308 (2002).

[7] L. Cameron, M. Footer, A. van Oudenaarden, and J. Theriot, Proc. Natl. Acad. Sci. U.S.A. **96**, 4908 (2000).

[8] D. Yarar, W. To, A. Abo, and M. Welch, Curr. Biol. **9**, 555 (1999).

[9] V. Noireaux, R.M. Golsteyn, E. Friederich, J. Prost, C. Antony, D. Louvard, and C. Sykes, Biophys. J. **78**, 1643 (2000).

[10] A. van Oudenaarden and J. Theriot, Nat. Cell Biol. **1**, 493 (1999).

[11] J. Taunton, B. Rowning, M. Coughlin, M. Wu, R. Moon, T. Mitchison, and C. Larabell, J. Cell Biol. **148**, 519 (2000).

[12] A. Upadhyaya, J. Chabot, A. Andreeva, A. Samadani, and A. van Oudenaarden, Proc. Natl. Acad. Sci. U.S.A. **100**, 4521 (2003).

[13] P.A. Giardini, D.A. Fletcher, and J.A. Theriot, Proc. Natl. Acad. Sci. U.S.A. **100**, 6493 (2003).

[14] J. Fradelizi, V. Noireaux, J. Plastino, B. Menichi, D. Louvard, C. Sykes, R. Golsteyn, and E. Friederich, Nat. Cell Biol. **3**, 699 (2001).

[15] For FITC (fluorescein isothiocyanate) labeling, VCA is incubated for 1 h with 0.08 mg/ml of FITC (in 100 mM borate buffer, pH 8.5) and dialysed against PBS at 4 C.

[16] H. Eyring, J. Chem. Phys. **3**, 107 (1935); H. A. Kramers, Physica (Utrecht) **7**, 284 (1940).

[17] Series of measurements in a given preparation of cell extract show a dispersion both in ℓ and v_p^0 of order ±20%. A much larger spread of several hundred percent is found between different preparations (leading to different total protein concentrations).